JREE: Vol. 9, No. 4, (Autumn 2022) 34-47

Journal of Renewable Energy and Environment

Journal Homepage: www.jree.ir

Materials and Energy Research Center

MERC

Research Article

The Problem of Resilient Stochastic Unit Commitment with Consideration of Existing Uncertainties Using the Rate of Change of Frequency

Moslem Geravandi, Hassan Moradi CheshmehBeigi *

Department of Electrical Engineering, Faculty of Engineering, Razi University, P. O. Box: 67144-14971, Kermanshah, Iran.

PAPER INFO

Paper history:
Received: 24 September 2021
Revised in revised form: 09 December 2021
Scientific Accepted: 08 January 2022
Published: 16 August 2022

Keywords:
Resilience,
Unit Commitment,
Uncertainty,
Wind and Solar Power Plants,
Load Interruption Contracts,
Adaptive Frequency Load Shedding

ABSTRACT

The ability of power systems against severe events shows their increased resilience, which in turn reduces the operation costs and recovery time of the system. This study presents a new resilient stochastic unit commitment model using the frequency change rate as a new index of system resilience. Furthermore, uncertainties of wind and solar power plants and demanded load are considered simultaneously. In the proposed method that considers the occurrence of a destructive incident in important production units in the worst-case scenarios and by using the generation capacity, adaptive frequency load shedding, and interrupting contracts, an effective strategy was provided to solve the unit commitment problem of thermal units to prevent instability in system frequency and to minimize unwanted load shedding. The proposed model was tested and evaluated on the IEEE 39-bus system with a wind power plant and a solar power plant. Moreover, the results obtained from simulation were reported. The effectiveness of this innovative approach in increasing the resilience of the power system against different degrees of uncertainty was confirmed based on the results.

https://doi.org/10.30501/jree.2022.306473.1262

1. INTRODUCTION

Nowadays, due to the depletion of conventional energy sources and emission of greenhouse gases, the use of wind and solar resources has increased significantly. Despite the many advantages of Wind and Solar Power Plants (WSPP), the output power of these sources is variable and cannot be predicted accurately. This issue has significant impact on the performance of power systems [1-3]. Unit Commitment Problem (UCP) is a complex multi-objective optimization problem employed to schedule the generation of the power system in the day-ahead given net load predictions and various operational constraints upon maintaining system security at a minimal cost [4, 5]. To meet this goal, the amount of load demand and WSPP must be predicted with maximum accuracy. The existence of many WSPPs in the power system causes high uncertainty in production scheduling [6]. Robust optimization and stochastic programming are two common frameworks for resolving uncertainties in the UCP. In the analysis of models using stochastic programming, uncertainty is shown through probability distribution [7, 8].

Severe events and destructive blackouts, in addition to the imposition of heavy damages, deprive many subscribers of access to electricity. In the past few years, a new concept called resilience in the electricity industry was considered by researchers, which is the boundary between system robustness and system reliability [9]. Resilience represents a set of capacities and capabilities that help the power system to operate with minimal damage and blackout in the event of a severe incident [10, 11]. Thus, despite the very low probability of such events due to the high costs imposed, extensive studies on the resilience of power systems independent of reliability studies are ongoing [12]. One of the new methods for evaluating the resilience of the power system in various studies is the use of graph theory. One advantage of this method is that the power system components can be represented as a graph and the system resilience is evaluated by studying the topological properties of the graph [13, 14]. In [15], a two-stage comparative robust formulation for microgrid disturbance scheduling was proposed considering various uncertainties using the column-constraint generation algorithm to minimize the destructive consequences of the islanding state. In [16], the fuzzy logic was employed to formulate a model in order to accurately predict the possible outage of equipment during severe incidents. In [17], a resilience-constrained day-ahead unit commitment model was presented using a decomposition algorithm based on the row-column production as a two-stage robust optimization problem to increase the system's resilience against extreme events.

In UCP, consumption-side management programs are of particular importance by setting up appropriate load-response

*Corresponding Author's Email: ha.moradi@razi.ac.ir (H. Moradi CheshmehBeigi)
URL: https://www.jree.ir/article_154881.html

Please cite this article as: Geravandi, M. and Moradi CheshmehBeigi, H., "The problem of resilient stochastic unit commitment with consideration of existing uncertainties using the rate of change of frequency", ***Journal of Renewable Energy and Environment (JREE)***, Vol. 9, No. 4, (2022), 34-47. (https://doi.org/10.30501/jree.2022.306473.1262).

contracts that aim to resolve problems such as balancing power and maintaining system frequency [18, 19]. In [20], the applications and types of microgrids were reviewed and the following economic studies and control of microgrids were explained. In [21], the imbalance between production and demand was studied using adaptive load shedding in the microgrids isolated from the grid considering uncertainties. This study respectively measured and evaluated the appropriate amount and location of load shedding without measuring the effect of load interruption contracts to maintain the system frequency in an acceptable range. In [22], the effect of the coordination between pumped storage and wind power plants considering the energy and reserve market on the normal and emergency performance (resilience) of the power system was investigated using integer linear combinational programming. In [23], a risk-constrained stochastic framework was employed to maximize the expected profit of a microgrid operator along with the uncertainties of renewable resources and demand. In this model, the balance between maximizing the operator's expected profit and the risk of receiving low profit in adverse scenarios was modeled using the conditional value at risk index and the impact of consumer participation in demand response programs.

In [24, 25], a method that considered the history of destructive hurricanes in the region and their path in the system for occurrence prediction was proposed in order to determine the units with outage risk. In [26], to reduce the effects of events on transmission lines in terms of time and place in the day-ahead market from a probabilistic perspective, the resilient UCP (R-UCP) was formulated as a distributionally robust optimization problem. One of the objectives of system automation is to use switching, which prevents the occurrence of events by taking necessary corrective actions [27]. Switching of transmission lines in UCP due to stress, physical tensions, and stability considerations within a limited time interval and in emergency such as a severe event that leads to line outage or congestion in other lines was investigated and evaluated [28]. In [29], to reduce the computational burden and solution time in UCP with several predicted line outages, the machine learning model was employed to determine the unnecessary constraints.

Given the above, most studies have not thoroughly studied the R-UCP because they failed to simultaneously consider uncertainties of WSPP and load demand, load interruption contracts, and adaptive frequency load shedding. As a result of previous research in this paper, WSPP is modeled as negative loads to ensure consistency with the basic concept of UCP, which is at the transmission voltage level. Also, due to the effects of WSPP on the power system, following the occurrence of an incident, improper WSPP conditions sometimes lead to the worsening of the system condition. Hence, the uncertainties of WSPP and load demand are considered to make more realistic decisions. Moreover, the effects of load interruption contracts and adaptive frequency load shedding on the system are evaluated. Then, by introducing an index for resilience, a resilient model is presented for the UCP. Finally, to demonstrate the effectiveness of the proposed R-UCP model, the proposed R-UCP is compared with the Traditional Two-Stage Stochastic Unit Commitment (TTSSUC) method combined with the load interruption contracts and adaptive frequency load shedding. Given the above, the innovations of this study are summarized as follows:

- Presentation of a new R-UCP model so that the working point of the system will change only in the event of a severe incident.
- Introduction of a new index to measure system resilience.
- Considering the effects of existing uncertainties on system resilience to make system operator decisions more realistic.
- Use of load management programs (adaptive frequency load shedding and load interruption contracts) and application of the production capacity to prevent instability in the system frequency and minimize the amount of unwanted load shedding.

The organization of this paper is as follows. In Section 2, the problem formulation is expressed. Section 3 describes the R-UCP solution method. Section 4 describes the result of numerical studies. Section 5 concludes the paper.

2. PROBLEM FORMULATION

2.1. Modeling the uncertainties of WSPP and load demand

As mentioned earlier, power generation using a power system with WSPP is subject to uncertainty. A well-known method for modeling uncertainty is the use of normal probability distribution functions [30]. In this research, by considering different forecasts for the WSPP power and load demand and using the prediction error probability distribution function with zero mean and different standard deviations, the value of uncertainties of WSPP power and load demand is obtained. According to the above, for the WSPP power or load demand, probable distributions with different standard deviations are considered. Each probable distribution is then divided into seventeen equal parts. In the following, seventeen error values are calculated relative to the mean value, with a specific probability for each error and standard deviation [31]. Therefore, seventeen prediction error modes are obtained with a specified probability for each mode of WSPP power or load demand. To combine different states of uncertainties of WSPP power and load demand and obtain the probability of each scenario, the scenario tree method is used in the proposed model. For each standard deviation and each WSPP power forecast error, there are seventeen load demand forecast errors. Therefore, 289 scenarios are developed for each standard deviation, taking into account all WSPP power prediction error modes. Based on the explanations given, there are a total of 4624 scenarios for all standard deviations. To ensure the robustness of the proposed model against changes in different input data, the average absolute error of the predicted data is considered to be ± 20 %.

2.2. Objective function

The objective function of resilient UCP, the value of which must be minimized, is represented by (1):

$$\min\{C^{UC} + C^{L.cut} + C^{L.sh}\} \quad (1)$$

where C^{UC} is the operation cost of the thermal units, which is defined in (2) considering the uncertainties, obtained using the two-stage stochastic programming method.

In the two-stage stochastic UCP, the on/off status decisions are fixed at the beginning of the day and production decisions are adapted to existing uncertainties [32-35].

$$C^{UC} = \sum_{t=1}^{T}\sum_{g=1}^{G}[(\sum_{\varphi=1}^{\phi} P_{\varphi}.(FC_{g,t,\varphi} + (e.E_{g,t,\varphi}))) + (SC_{g,t}.U_{g,t}.(1-U_{g,t-1})) + (DC_{g,t}.U_{g,t-1}.(1-U_{g,t}))] \quad (2)$$

where $FC_{g,t}$ is the fuel cost function of unit g at hour t and $E_{g,t}$ is the emission function of unit g at hour t, as expressed in (3) and (4).

$$FC_{g,t,\varphi} = U_{g,t}.(a_g + b_g P_{g,t,\varphi} + c_g P_{g,t,\varphi}^2) \quad \forall g \in G, t \in T, \forall \varphi \in \phi \quad (3)$$

$$E_{g,t,\varphi} = U_{g,t}.(\alpha_g + \beta_g P_{g,t,\varphi} + \gamma_g P_{g,t,\varphi}^2) \quad \forall g \in G, t \in T, \forall \varphi \in \phi \quad (4)$$

The startup cost SCg, depending on the hours when the unit g is off, is equal to one of the hot or cold startup costs as expressed in (5).

$$SC_g = \begin{cases} HSC_g & \text{if } DT_g \le CSH_g \\ CSC_g & \text{if } DT_g \succ CSH_g \end{cases} \quad (5)$$

The load costs consist of two parts: load interruption cost expressed in (6) and the cost resulting from adaptive frequency load shedding expressed in (7).

$$C^{L.cut} = \sum_{t=1}^{T}\sum_{\varphi=1}^{\phi} e_{L.cut}.P_{\varphi}.P_{t,\varphi}^{L.cut} \quad (6)$$

$$C^{L.sh} = \sum_{t=1}^{T}\sum_{\varphi=1}^{\phi} e_{L.sh}.P_{\varphi}.P_{t,\varphi}^{L.sh} \quad (7)$$

where $C^{L.cut}$ denotes the load interruption contracts cost in which $e_{L.cut}$ is the cost coefficient of load interruption according to the contract concluded with the participants in these programs. This cost coefficient during low load hours has its minimum value, while it has its maximum value during critical and peak hours. In addition, $C^{L.sh}$ shows the cost of adaptive frequency load shedding in which $e_{L.sh}$ is the cost coefficient of load shedding. This cost coefficient during low load hours has its minimum value and has its maximum value during critical and peak hours.

ΔP^H is a negative value that indicates the lack of active power for each scenario at each hour after the incident and can be calculated according to (8) [18, 36]:

$$\Delta P^H = (\sum_{g=1}^{G} P_{g,t,\varphi}) - P_{t,\varphi}^D + P_{w,t,\varphi} + P_{s,t,\varphi} \quad (8)$$

Equation (9) shows the load interruption value of the existing demand for each scenario per hour in the load interruption contracts to adjust the system frequency.

$$\Delta P_{L.cut}^H = -\Delta P^H \quad (9)$$

Equation (10) shows the unwanted load shedding value of the existing demand for each scenario per hour in the adaptive frequency load shedding to adjust the system frequency.

$$\Delta P_{L.sh}^H = -\Delta P^H - \Delta P_{L.cut}^H \quad (10)$$

In this paper, the rate of frequency change is introduced as a new index for measuring the resilience of the system [18, 36]. Equation (11) shows how to calculate the value of system frequency variations.

$$\frac{d\varpi_{el}}{dt} = \frac{\Delta P^H}{2H_{sys}} \times \varpi_{el} \quad (11)$$

2.3. Problem constraints

The main constraints of the UCP can be generally divided into two categories of equal and unequal constraints, which are expressed in (12) to (19) [32-35].

Power balance and spinning reserve constraints:

$$\sum_{g=1}^{G} P_{g,t,\varphi}.U_{g,t} = P_{t,\varphi}^D - P_{w,t,\varphi} - P_{s,t,\varphi} - P_{t,\varphi}^{L.cut} - P_{t,\varphi}^{L.sh} \quad \forall g \in G, \forall t \in T, \forall \varphi \in \phi \quad (12)$$

$$\sum_{g=1}^{G} P_g^{max}.U_{g,t} \ge P_{t,\varphi}^D - P_{w,t,\varphi} - P_{s,t,\varphi} - P_{t,\varphi}^{L.cut} - P_{t,\varphi}^{L.sh} + SR_{t,\varphi} \quad \forall g \in G, \forall t \in T, \forall \varphi \in \phi \quad (13)$$

$$SR_{t,\varphi} = 0.05P_{t,\varphi}^D \quad \forall t \in T, \forall \varphi \in \phi \quad (14)$$

Output power constraint of unit g at time t and scenario φ:

$$P_g^{min} \le P_{g,t,\varphi} \le P_g^{max} \quad \forall g \in G, \forall t \in T, \forall \varphi \in \phi \quad (15)$$

Constraints related to ramp-up/ramp-down and startup/shutdown limitation of unit g:

$$P_{g,t,\varphi} - P_{g,t-1,\varphi} \le SU_g(U_{g,t} - U_{g,t-1}) + RU_g.U_{g,t-1} \quad \forall g \in G, \forall t \in T, \forall \varphi \in \phi \quad (16)$$

$$P_{g,t-1,\varphi} - P_{g,t,\varphi} \le SD_g(U_{g,t-1} - U_{g,t}) + RD_g.U_{g,t} \quad \forall g \in G, \forall t \in T, \forall \varphi \in \phi \quad (17)$$

Constraints related to a minimum on/off time of unit g:

$$U_{g,t} - U_{g,t-1} \le U_{g,\tau} \quad \forall g \in G, \forall t \in T, \forall \tau \in \{t+1, ..., \min\{t, UT_g, T\}\} \quad (18)$$

$$U_{g,t-1} - U_{g,t} \le 1 - U_{g,\tau} \quad \forall g \in G, \forall t \in T, \forall \tau \in \{t+1, ..., \min\{t, DT_g, T\}\} \quad (19)$$

3. THE UCP SOLUTION METHOD

The proposed R-UCP model for scheduling thermal units is a hybrid model that has been proposed to increase the system resilience and minimize unwanted load shedding during a severe incident.

3.1. Proposed model algorithm

Figure 1 shows the flowchart of the R-UCP algorithm. Initially, by solving the UCP for system operation in the normal mode for all scenarios, considering all the constraints and uncertainties using two-stage stochastic programming, production information and scheduling of units are obtained. Then, the information of the studied scenarios, including the time of occurrence of incidents and the number of units that have been outages due to the incidents, is received as input.

After the incident, to use the production capacity by modifying the scheduling table of the thermal units in each hour after the incident with emphasis on all the constraints, the units that are online and produce power with a fraction of the nominal capacity, their capacity is increased up to the allowable limit. If the lack of production capacity is not

resolved, the thermal units that are off every hour after the incident and are allowed to operate will be turned on to overcome the system inertia and reduce production capacity. If the production capacity cannot overcome the lost capacity, load interruption programs, which consist of load interruption contracts, are implemented. If the dimensions of the incident are wider and the production capacity and load interruption programs cannot overcome the reduction in production capacity, adaptive frequency load shedding is used to balance the power in the system. If the system frequency does not reach its allowable range, it is not logical to maintain the system in its integrated form and the operator must command to prevent further failure in the islanding state.

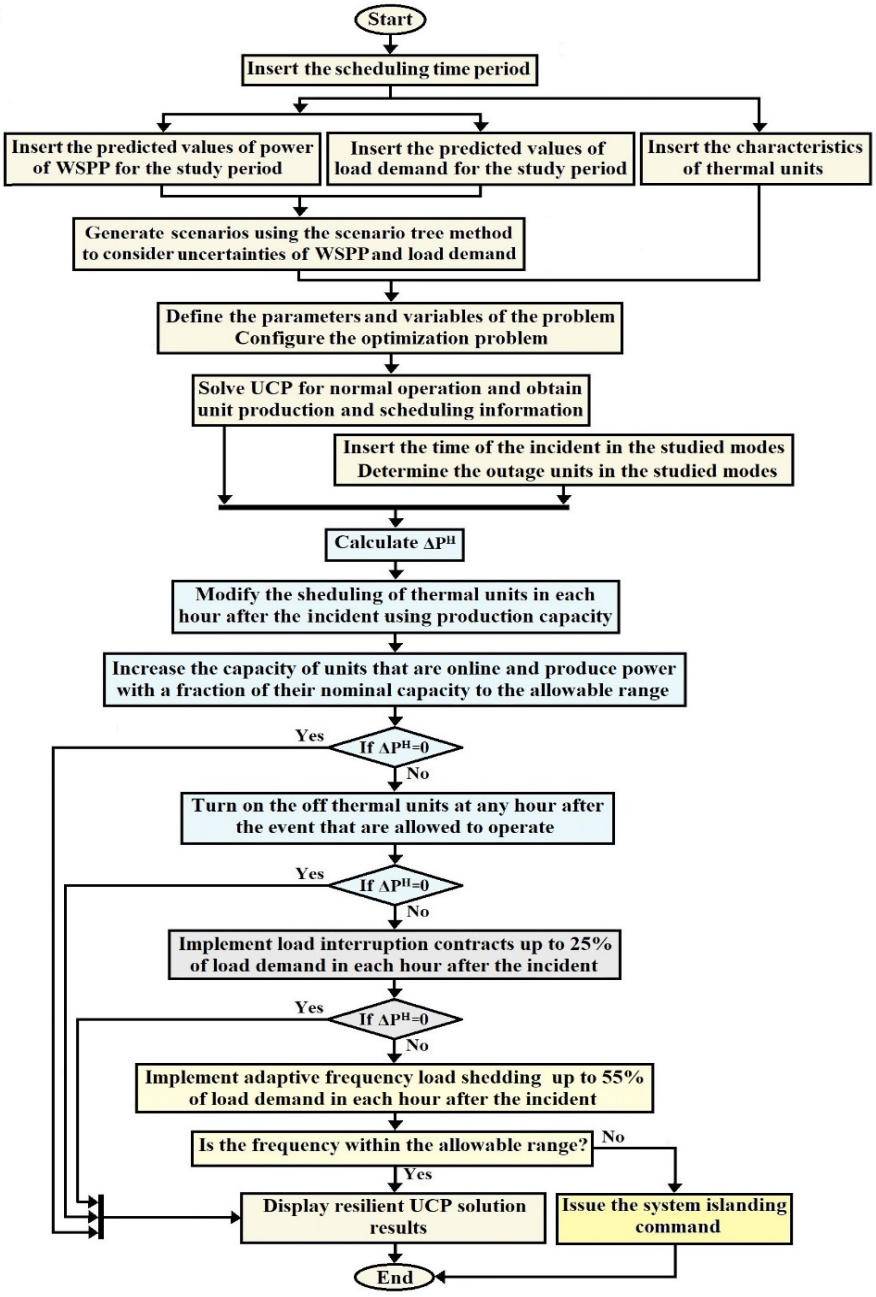

Figure 1. Algorithm of the proposed R-UCP model

3.2. Load interruption contracts and adaptive frequency load shedding

In this paper, to increase system resilience, load interruption contracts are considered as flexible resources. Load interruption contracts are concluded before the occurrence of events between the volunteer loads and the system operator. These loads are prioritized for cut-off by receiving rewards from the system operator. These concessions are modeled in the form of fees paid to subscribers participating in load interruption programs. If the thermal units (production capacity) cannot overcome the lost capacity, load interruption contracts are implemented. The number of load interruption contracts at each hour is assumed to be up to 25 % of the total demand at that hour. The cost of payment for the participating loads is calculated using (6). Finally, adaptive frequency load shedding has been considered the last approach to dealing with frequency decline.

According to (11), the frequency change rate is directly related to the reduction of active power in the system. Therefore, to maintain the system frequency, the value of active power reduction (ΔP^H) must be zero. At this stage,

assuming that all production capacity and load interruption sources are used, the required amount of frequency load shedding is performed to stabilize the frequency. The cost of blackout damage due to adaptive frequency load shedding is calculated using (7). The value of frequency load shedding to adjust the system frequency can be calculated using (10). The value of load shedding in adaptive frequency load shedding at each hour is assumed to be up to 55 % of the total demand at that hour. In case of the inability of this solution to stabilize the system frequency and force the operator to eliminate more than 80 % of the system demand, islanding will be a higher priority.

4. NUMERICAL STUDIES

The R-UCP model was evaluated on the 39-bus IEEE test system with the WSPP. This system has ten thermal units. Specifications of thermal units and the amount of load demand are presented in Table 1 and Figure 2 [37, 38]. The mean predicted output power of WSPP connected to the system at each hour is presented in Figure 2 [39-41]. The cost of producing each ton of emission by thermal units is assumed to be 0.05 $, and the amount of spinning reserve at each hour is assumed to be 0.05 times the load demand at that hour. The cost coefficient of load interruption contracts for different hours is presented in Table 2. The cost coefficient of adaptive frequency load shedding is assumed to be 130 % of the cost coefficient of load interruption contracts for different hours [42].

The probability of each prediction error of WSPP power or load demand for different standard deviations is shown in Table 3. Each time interval is considered equal to one hour, and the total scheduling time is one day. For a comprehensive review of the proposed model, the peak load demand time is selected as the worst time of the incident and case studies are reviewed and evaluated at this time. The case studies here are categorized in Table 4. For each case study, in the case of every standard deviation of the prediction error of WSPP and load according to the scenario tree method, 289 scenarios are defined. Therefore, for all prediction errors and standard deviations, a total of 4624 scenarios are obtained. To guarantee the robustness of the simulation results, the average absolute error of the predicted data is considered to be 20 %. All calculations are performed in a MATLAB environment with a machine running at Intel(R) Core (TM) i5-8250u 1.6 GHz CPU and 8GB RAM.

Table 1. Specifications of thermal units [37, 38]

	Unit 1	Unit 2	Unit 3	Unit 4	Unit 5	Unit 6	Unit 7	Unit 8	Unit 9	Unit 10
P_{max} (MW)	455	455	130	130	160	80	85	55	55	55
P_{min} (MW)	150	150	20	20	25	20	25	10	10	10
UT (h)	8	8	5	5	6	3	3	1	1	1
DT (h)	8	8	5	5	6	3	3	1	1	1
Initial state (h)	+8	+8	-5	-5	-6	-3	-3	-1	-1	-1
a ($/h)	1000	970	700	680	450	370	480	660	665	670
b ($/MWh)	16	17	16	16	19	22	27	25	27	27
c ($/MW^{2}h)	0.00048	0.00031	0.0020	0.0021	0.00398	0.00712	0.00079	0.00413	0.0022	0.00173
HSC ($/h)	4500	5000	550	560	900	170	260	30	30	30
CSC ($/h)	9000	10000	1100	1120	1800	340	520	60	60	60
CSH (h)	5	5	4	4	4	2	2	0	0	0
DC ($/h)	4500	5000	550	560	900	170	260	30	30	30
RU	225	225	50	50	60	60	60	135	135	135
RD	455	455	130	130	160	80	85	55	55	55
SU	150	150	20	20	25	20	25	10	10	10
SD	150	150	20	20	25	20	25	10	10	10
α (ton/h)	10.33908	10.33908	30.0391	30.0391	32.00006	32.00006	33.00056	33.00056	35.00056	36.00012
β (ton/MWh)	-0.24444	-0.24444	-0.40695	-0.40695	-0.38132	-0.38132	-0.39023	-0.39023	-0.39524	-0.39864
γ (ton/ MW^{2}h)	0.00312	0.00312	0.00509	0.00509	0.00344	0.00344	0.00465	0.00465	0.00465	0.00470

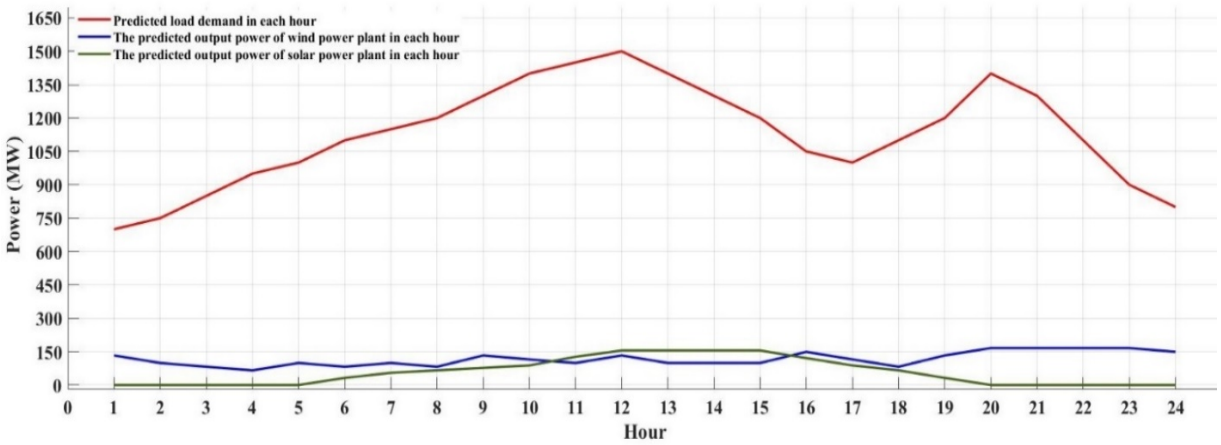

Figure 2. Predicted values of load demand and output power of wind and solar power plants per hour [37, 39-41]

Table 2. The cost coefficient of load interruption contracts [42]

Hour	1	2	3	4	5	6	7	8	9	10	11	12	13	14	15	16	17	18	19	20	21	22	23	24
Cost ($)	14	14	14	14	14	14	14	17	17	17	17	27	27	27	27	17	17	17	27	27	27	27	14	14

Table 3. The probability of each prediction error of WSPP power or load demand for different standard deviations

		Probability of prediction error for standard deviation= 0.025	Probability of prediction error for standard deviation= 0.050	Probability of prediction error for standard deviation= 0.075	Probability of prediction error for standard deviation= 0.100
Percentage prediction error	20.0 %	0	0.0001	0.0024	0.0076
	17.5 %	0	0.0005	0.0089	0.0217
	15.0 %	0	0.0024	0.0182	0.0325
	12.5 %	0	0.0092	0.0334	0.0457
	10.0 %	0.0002	0.0278	0.0549	0.0605
	7.5 %	0.006	0.0656	0.0807	0.0752
	5.0 %	0.0606	0.1210	0.1062	0.0878
	2.5 %	0.2417	0.1747	0.1253	0.0964
	0.0 %	0.383	0.1974	0.14	0.1452
	-2.5 %	0.2417	0.1747	0.1253	0.0964
	-5.0 %	0.0606	0.1210	0.1062	0.0878
	-7.5 %	0.006	0.0656	0.0807	0.0752
	-10.0 %	0.0002	0.0278	0.0549	0.0605
	-12.5 %	0	0.0092	0.0334	0.0457
	-15.0%	0	0.0024	0.0182	0.0325
	-17.5 %	0	0.0005	0.0089	0.0217
	-20.0 %	0	0.0001	0.0024	0.0076

Table 4. Case studies

		Disconnected WPSS and thermal units
Case	1	Simultaneous outage of G1, WSPP
	2	Simultaneous outage of G1, G2
	3	Simultaneous outage of G1, G2, G5, Solar power plant

Initially, the UCP is solved through two-stage stochastic programming and based on all operational constraints and uncertainties for the normal operation mode during the operation period. Table 5 shows the scheduling table of the thermal units for a sample scenario in the entire operation period for both R-UCP and TTSSUC methods. It should be noted that both R-UCP and TTSSUC methods are quite similar for the normal operation mode and in the hours before the incident.

Table 5. Scheduling table of thermal units for a sample scenario in the whole operation period for the normal operation mode

		Production power of thermal units (MW)									
		G1	G2	G3	G4	G5	G6	G7	G8	G9	G10
Hour	1	455	278.6	0	0	0	0	0	0	0	0
	2	455	345.8	20	0	0	0	0	0	0	0
	3	455	434.4	20	20	25	0	0	0	0	0
	4	455	455	70	70	37.2	0	0	0	0	0
	5	455	455	120	45.8	25	20	0	0	0	0
	6	455	455	130	95.8	73	20	0	0	0	0
	7	455	455	130	130	66.8	20	0	0	0	0
	8	455	455	130	130	121.6	20	0	10	0	0
	9	455	455	130	130	157	20	25	10	10	0
	10	455	455	130	130	160	80	32.6	55	10	10
	11	455	455	130	130	160	80	74.2	55	10	10
	12	455	455	130	130	160	80	84.6	55	10	10
	13	455	455	130	130	160	80	25	21.8	10	10
	14	455	455	130	130	131.8	20	25	10	0	0
	15	455	455	130	130	46.8	20	0	0	0	0
	16	455	455	69	20	25	20	0	0	0	0
	17	455	455	62.6	20	25	20	0	0	0	0
	18	455	455	112.6	70	85	24	0	0	0	0
	19	455	455	130	120	73	20	25	10	10	10
	20	455	455	130	130	133	80	85	55	14.2	10
	21	455	455	130	130	160	42.2	25	10	10	10
	22	455	455	130	92.2	25	20	0	10	0	0
	23	455	427.2	20	20	25	0	0	0	0	0
	24	455	365.8	20	0	0	0	0	0	0	0

According to Table 5, two important thermal units with high production capacity (G1, G2) are on due to the low cost of production during the whole operation period. Also, at hours 10 to 13 and 19 to 21, which is the peak of load demand, it is observed that all thermal units are online to meet the load demand and spinning reserve. On the other hand, the total operation cost of the system, taking into account not only all constraints during 24 hours but also uncertainties, is 513042 $ and without considering uncertainties is 512923 $. As stated earlier, the total operation cost of the system in the mode with uncertainty is 0.023 % higher than that in the mode without uncertainty, which can be concluded that in calculating the total operation cost of the system, uncertainties have minor impact. According to the load demand, the system has the highest load demand at 12 o'clock. Therefore, to evaluate the performance of the proposed R-UCP, peak demand time is selected as the worst time occurrence of the incident and case studies are evaluated at this time.

4.1. Case study 1

In Case Study 1, with the simultaneous outage of thermal unit G1 and WSPP at 12 o'clock, 27.4 % of the production capacity of thermal units and total WSPP production capacity are lost. In this case, the proposed R-UCP model is solved to prevent system frequency instability and minimize unwanted load shedding. Table 6 shows the modified scheduling table of the thermal units of the system, taking into account all the constraints and existing uncertainties for a sample scenario at each hour during the operation period using the R-UCP method. According to Table 6, it can be seen that after the occurrence of the incident at the peak load time, to use the production capacity to compensate for the lost capacity, the scheduling of the thermal units was modified every hour after the incident. In the hours after the incident, the units that are on and produce power with a fraction of their nominal capacity, according to all the constraints, their capacity will increase to the allowable range. If the lack of production capacity is not compensated, the thermal units that are off and allowed to operate are turned on and committed.

As can be seen in Table 6, blue houses in the schedule table are thermal units that are on in the hours after the incident and their production capacity has increased compared to the normal state in order to overcome the lost capacity. In addition, the red houses in the scheduling table are off thermal units that allowed to turn on in the hours after the incident. These units are turned on and committed in the hours after the incident to resolve the issue of the lost capacity.

Table 7 shows the values of load interruption in load interruption contracts as well as load shedding in adaptive frequency load shedding for each hour after the incident in the case of the proposed R-UCP and TTSSUC methods. According to Table 7, it is observed that in the proposed R-UCP method in modes with and without uncertainty, the value of load interruption in most hours after the incident is much lower than the TTSSUC method. Also, in the proposed R-UCP method in modes with and without uncertainty, the value of unwanted load shedding in most hours after the incident is equal to zero or a small value. However, in the TTSSUC method, in modes with and without uncertainty, the value of unwanted load shedding at hours 23 and 24 is large. Therefore, in Case Study 1, the proposed R-UCP model, unlike the TTSSUC, has successfully prevented unwanted load shedding in all hours after the incident by using production capacity and load side management programs.

Table 6. Modified scheduling table of thermal units for a sample scenario in the case of the proposed R-UCP method in the whole operation period for Case Study 1

		Production power of thermal units (MW)									
		G1	G2	G3	G4	G5	G6	G7	G8	G9	G10
Hour	1	455	278.6	0	0	0	0	0	0	0	0
	2	455	345.8	20	0	0	0	0	0	0	0
	3	455	434.4	20	20	25	0	0	0	0	0
	4	455	455	70	70	37.2	0	0	0	0	0
	5	455	455	120	45.8	25	20	0	0	0	0
	6	455	455	130	95.8	73	20	0	0	0	0
	7	455	455	130	130	66.8	20	0	0	0	0
	8	455	455	130	130	121.6	20	0	10	0	0
	9	455	455	130	130	157	20	25	10	10	0
	10	455	455	130	130	160	80	32.6	55	10	10
	11	455	455	130	130	160	80	74.2	55	10	10
	12	outage	455	130	130	160	80	85	55	55	10
	13	outage	455	130	130	160	80	85	55	55	10
	14	outage	455	130	130	160	80	85	55	55	55
	15	outage	455	130	130	160	80	85	55	55	55
	16	outage	455	130	130	160	80	85	55	55	55
	17	outage	455	130	130	160	80	85	55	55	55
	18	outage	455	130	130	160	80	85	55	55	55
	19	outage	455	130	130	160	80	85	55	55	55
	20	outage	455	130	130	160	80	85	55	55	55
	21	outage	455	130	130	160	80	85	55	55	55
	22	outage	455	130	130	160	80	85	55	55	55
	23	outage	455	130	130	160	80	50	55	10	10
	24	outage	455	130	130	160	50	25	10	0	0

Table 7. The value of load interruption in load interruption contracts and that of load shedding in adaptive frequency load shedding for each hour after the incident in Case Study 1 for TTSSUC and proposed R-UCP methods

		Hour												
		12	13	14	15	16	17	18	19	20	21	22	23	24
The value of load interruption in load interruption contracts at each hour after the incident (MW)	R-UCP method with uncertainty	289.8	195.4	100.7	25.82	0.39	0	2.71	25.82	195.4	100.7	2.66	0	0
	TTSSUC method with uncertainty	289.8	278.8	293.3	239.6	97.97	53.71	145.6	189.3	195.4	241.6	193.1	221.4	192
	R-UCP method without uncertainty	295	195	95	0	0	0	0	0	195	95	0	0	0
	TTSSUC method without uncertainty	295	285	310	245	95	45	145	190	195	245	195	225	200
The value of unwanted load shedding in adaptive frequency load shedding at each hour after the incident (MW)	R-UCP method with uncertainty	5.2	0.39	0	0	0	0	0	0	0.39	0	0	0	0
	TTSSUC method with uncertainty	5.2	6.2	16.69	5.4	0	0	0.2	0.93	0.39	3.43	1.9	48.53	23.01
	R-UCP method without uncertainty	0	0	0	0	0	0	0	0	0	0	0	0	0
	TTSSUC method without uncertainty	0	0	0	0	0	0	0	0	0	0	0	45	15

Table 8 shows the operation cost of the system and the operation cost of the thermal units in the entire period of operation as well as the costs of load interruption contracts and adaptive frequency load shedding for hours after the incident for both TTSSUC and proposed R-UCP methods. The value of the operation cost of the system, taking into account all the constraints during 24 hours, is equal to the sum of the operation cost of the thermal units, costs of load interruption contracts, and costs from adaptive frequency load shedding. In the proposed R-UCP method, the value of the operation cost of the system during 24 hours is 599754 $ for the mode with uncertainty and 599392 $ for the mode without uncertainty, which is 16.9 % higher than the normal operation mode. In the TTSSUC method, the value of the operation cost of the system during 24 hours is 579565$ for the mode with uncertainty and 579216$ for the mode without uncertainty, which is 12.9 % higher than the normal operation mode. Considering that 27.4 % of the production capacity of thermal units and total WSPP production capacity has been lost following the occurrence of an incident during peak hour, the proposed R-UCP model with only a 16.9 % increase in the operation cost of the system compared to normal operation has effectively prevented the frequency instability and unwanted load shedding in the system, which is quite satisfactory. Although the operation cost of the system in the TTSSUC method is about 20,000$ less than that in the proposed R-UCP method, it should be noted that in the event of an incident, the main objective is to reduce unwanted load shedding rather than the operation cost of the system.

Table 8. The operation cost of the system and that of the thermal units in the entire period of operation as well as the costs of load interruption contracts and adaptive frequency load shedding in the hours after the accident in Case Study 1 for both TTSSUC and proposed R-UCP methods

		R-UCP method				TTSSUC method			
		The operation cost of the system	The operation cost of the thermal units	The costs of load interruption contracts	The costs due to adaptive frequency load shedding	The operation cost of the system	The operation cost of the thermal units	The costs of load interruption contracts	The costs due to adaptive frequency load shedding
cost ($)	With uncertainty	599754	574213	25331	210	579565	514138	62711	2716
	Without uncertainty	599392	575767	23625	0	579216	514409	63715	1092

According to the results obtained from Case Study 1, in the case of the proposed R-UCP method, unlike the TTSSUC method in the hours after the incident, all the allowable capacity of the turned-on units is utilized. In addition, in the proposed R-UCP method, in the hours after the incident, the off thermal units that are allowed to be operated are terned on and committed. Unlike the TTSSUC method, given that much of the lost capacity is compensated by the thermal units in the proposed R-UCP method, the unwanted load shedding is lower than that in the TTSSUC method. The reason for increasing the operating cost of the system in the R-UCP method compared to the TTSSUC method is the use of more thermal units and costs resulting from emission.

4.2. Case study 2

In Case Study 2, with the simultaneous outage of thermal units G1, G2 at 12 o'clock, 54.82 % of the production capacity of thermal units is lost. Table 9 shows the modified scheduling table of the thermal units of the system, considering all the constraints and existing uncertainties for a sample scenario for each hour during the operation period using the R-UCP method. According to Table 9, similar to Case Study 1, it is observed that after the occurrence of an incident at peak hour, to use the production capacity to overcome the lost capacity, scheduling the thermal units at each hour after the incident was modified. In this case,

compared to the normal mode, blue houses in the scheduling table were the units that were on in the hours after the incident and their production capacity increased, while red houses in the scheduling table were off units which were allowed to go on in the hours after the incident and were turned on and committed after the incident.

Table 9. Modified scheduling table of thermal units for a sample scenario for the proposed R-UCP method in the whole operation period for Case Study 2

		Production power of thermal units (MW)									
		G1	G2	G3	G4	G5	G6	G7	G8	G9	G10
Hour	1	455	278.6	0	0	0	0	0	0	0	0
	2	455	345.8	20	0	0	0	0	0	0	0
	3	455	434.4	20	20	25	0	0	0	0	0
	4	455	455	70	70	37.2	0	0	0	0	0
	5	455	455	120	45.8	25	20	0	0	0	0
	6	455	455	130	95.8	73	20	0	0	0	0
	7	455	455	130	130	66.8	20	0	0	0	0
	8	455	455	130	130	121.6	20	0	10	0	0
	9	455	455	130	130	157	20	25	10	10	0
	10	455	455	130	130	160	80	32.6	55	10	10
	11	455	455	130	130	160	80	74.2	55	10	10
	12	outage	outage	130	130	160	80	85	55	55	10
	13	outage	outage	130	130	160	80	85	55	55	10
	14	outage	outage	130	130	160	80	85	55	55	55
	15	outage	outage	130	130	160	80	85	55	55	55
	16	outage	outage	130	130	160	80	85	55	55	55
	17	outage	outage	130	130	160	80	85	55	55	55
	18	outage	outage	130	130	160	80	85	55	55	55
	19	outage	outage	130	130	160	80	85	55	55	55
	20	outage	outage	130	130	160	80	85	55	55	55
	21	outage	outage	130	130	160	80	85	55	55	55
	22	outage	outage	130	130	160	80	85	55	55	55
	23	outage	outage	130	130	160	80	85	55	55	55
	24	outage	outage	130	130	160	50	85	55	55	55

Table 10 shows the values of load interruption in load interruption contracts and load shedding in adaptive frequency load shedding for each hour after the incident in the case of the proposed R-UCP and TTSSUC methods. According to Table 10, it is observed that in the proposed R-UCP method in modes with and without uncertainty, the values of load interruption and load shedding in most hours after the incident are much less than those in the TTSSUC method. According to Table 10, for the TTSSUC method, in modes with and without uncertainty, the entire capacity of load interruption contracts is utilized in all hours after the incident. However, in the proposed R-UCP method, the entire capacity of load interruption contracts is used at some hours. Therefore, due to the high volume of production capacity lost for modes with and without uncertainty, the proposed R-UCP method, unlike the TTSSUC method, successfully prevents large unwanted load shedding in the hours after the incident.

Table 10. The value of load interruption in load interruption contracts and the value of load shedding in adaptive frequency load shedding for each hour after the incident in Case Study 2 for TTSSUC and proposed R-UCP methods

		Hour												
		12	13	14	15	16	17	18	19	20	21	22	23	24
The value of load interruption in load interruption contracts in each hour after the incident (MW)	R-UCP method with uncertainty	370.2	340.1	283.2	194.9	44.09	55.67	199.5	269.7	349	318.9	182.8	14.92	0.85
	TTSSUC method with uncertainty	370.2	349	325	299.8	249.8	245.4	275	300	349	325	275	225	200
	R-UCP method without uncertainty	375	350	296	196	30	47	202	285	350	325	184	0	0
	TTSSUC method without uncertainty	375	350	325	300	262.5	250	275	300	350	325	275	225	200
The value of unwanted load shedding in adaptive frequency load shedding in each hour after the incident (MW)	R-UCP method with uncertainty	91.78	55.92	12.76	1.34	0	0	2.53	15.28	134.9	65.06	1.36	0	0
	TTSSUC method with uncertainty	91.78	136.9	186	146.2	30.18	51.62	177	180	134.9	209	209	334	321
	R-UCP method without uncertainty	87	46	0	0	0	0	0	0	134	59	0	0	0
	TTSSUC method without uncertainty	87	136	186	146	17.5	47	177	180	134	209	209	334	321

Table 11 shows the operation cost of the system and the operation cost of the thermal units in the entire period of operation, and the costs of load interruption contracts and adaptive frequency load shedding for hours after the incident for both TTSSUC and proposed R-UCP methods. In the proposed R-UCP method, the value of the operation cost of the system during 24 hours is 572430 $ for the mode with uncertainty and 572348 $ for the mode without uncertainty, which is 11.56 % higher than the normal operation mode. In the TTSSUC method, the value of the operation cost of the system during 24 hours is 552239 $ for the mode with uncertainty and 552025 $ for the mode without uncertainty, which is 7.64 % higher than the normal operation mode. Similar to Case Study 1, the reason for the increased operating cost of the system in the proposed R-UCP method compared to the TTSSUC method is the emission-related costs. The reason for the lower operating cost of the system in Case Study 2 compared to Case Study 1 is the existence of WSPP and the supply of a part of the demand by it.

Table 11. The operation cost of the system and the operation cost of the thermal units in the entire period of operation and the costs of load interruption contracts and adaptive frequency load shedding in the hours after the accident in Case Study 2 for both TTSSUC and proposed R-UCP methods

		R-UCP method				TTSSUC method			
		The operation cost of the system	The operation cost of the thermal units	The costs of load interruption contracts	The costs due to adaptive frequency load shedding	The operation cost of the system	The operation cost of the thermal units	The costs of load interruption contracts	The costs due to adaptive frequency load shedding
cost ($)	With uncertainty	572430	491440	67649	13341	552239	400125	89055	63059
	Without uncertainty	572348	492415	68490	11443	552025	400056	89537	62432

4.3. Case study 3

In Case Study 3, with the simultaneous outage of thermal units G1, G2, G5 and solar power plant at 12 o'clock, 64.45 % of the production capacity of thermal units and total solar power plant production capacity are lost. Table 12 shows the modified scheduling table of the thermal units of the system, considering all the constraints and existing uncertainties for a sample scenario for each hour during the operation period using the R-UCP method. In the case of Study 3, as in Case Studies 1 and 2, it is observed that after the occurrence of an incident at peak hour, to use the production capacity to compensate for the lost capacity, scheduling the thermal units at each hour after the incident has been modified.

Table 12. Modified scheduling table of thermal units for a sample scenario for the proposed R-UCP method in the whole operation period for Case Study 3.

		Production power of thermal units (MW)									
		G1	G2	G3	G4	G5	G6	G7	G8	G9	G10
Hour	1	455	278.6	0	0	0	0	0	0	0	0
	2	455	345.8	20	0	0	0	0	0	0	0
	3	455	434.4	20	20	25	0	0	0	0	0
	4	455	455	70	70	37.2	0	0	0	0	0
	5	455	455	120	45.8	25	20	0	0	0	0
	6	455	455	130	95.8	73	20	0	0	0	0
	7	455	455	130	130	66.8	20	0	0	0	0
	8	455	455	130	130	121.6	20	0	10	0	0
	9	455	455	130	130	157	20	25	10	10	0
	10	455	455	130	130	160	80	32.6	55	10	10
	11	455	455	130	130	160	80	74.2	55	10	10
	12	outage	outage	130	130	outage	80	85	55	55	10
	13	outage	outage	130	130	outage	80	85	55	55	10
	14	outage	outage	130	130	outage	80	85	55	55	55
	15	outage	outage	130	130	outage	80	85	55	55	55
	16	outage	outage	130	130	outage	80	85	55	55	55
	17	outage	outage	130	130	outage	80	85	55	55	55
	18	outage	outage	130	130	outage	80	85	55	55	55
	19	outage	outage	130	130	outage	80	85	55	55	55
	20	outage	outage	130	130	outage	80	85	55	55	55
	21	outage	outage	130	130	outage	80	85	55	55	55
	22	outage	outage	130	130	outage	80	85	55	55	55
	23	outage	outage	130	130	outage	80	85	55	55	55
	24	outage	outage	130	130	outage	50	85	55	55	55

Table 13 shows the values of load interruption in load interruption contracts and load shedding in adaptive frequency load shedding for each hour after the incident for the proposed R-UCP and TTSSUC methods. According to Table 13, it is observed that in the TTSSUC and proposed R-UCP methods in modes with and without uncertainty, the value of load interruption is equal in most hours after the incident. The proposed R-UCP method uses the full capacity of the load

interruption contracts except at hours 23 and 24, while the TTSSUC method uses the full capacity of the load interruption contracts in all hours after the incident. Also, it is observed that in the proposed R-UCP method in modes with and without uncertainty, the value of load shedding in most hours after the incident is much less than that in the case of the TTSSUC method. Therefore, similar to the previous case studies, due to the high volume of production capacity lost for modes with and without uncertainty, the proposed R-UCP method, unlike the TTSSUC method, successfully prevents large unwanted load shedding in the hours after the incident.

Table 13. The value of load interruption in load interruption contracts and the value of load shedding in adaptive frequency load shedding for each hour after the incident in Case Study 3 for TTSSUC and proposed R-UCP methods

		Hour												
		12	13	14	15	16	17	18	19	20	21	22	23	24
The value of load interruption in load interruption contracts in each hour after the incident (MW)	R-UCP method with uncertainty	375	350	325	300	257.7	245.3	275	300	350	325	272.1	143.3	64.37
	TTSSUC method with uncertainty	375	350	325	300	262.5	250	275	300	350	325	275	225	200
	R-UCP method without uncertainty	375	350	325	300	262.5	250	275	300	350	325	275	144	61
	TTSSUC method without uncertainty	375	350	325	300	262.5	250	275	300	350	325	275	225	200
The value of unwanted load shedding in adaptive frequency load shedding in each hour after the incident (MW)	R-UCP method with uncertainty	402	361	286	211	53.3	49.7	153	177	294	219	71.9	0.85	0
	TTSSUC method with uncertainty	402	401	501	461	298.5	295	403	372	294	369	369	359	321
	R-UCP method without uncertainty	402	361	286	211	48.5	45	153	177	294	219	69	0	0
	TTSSUC method without uncertainty	402	401	501	461	298.5	295	403	372	294	369	369	359	321

Table 14 shows the operation cost of the system and the operation cost of the thermal units in the entire period of operation as well as the costs of load interruption contracts and adaptive frequency load shedding for hours after the incident for both TTSSUC and proposed R-UCP methods. In the proposed R-UCP method, the value of the operation cost of the system during 24 hours is 612371 $ for the mode with uncertainty and 612037 $ for the mode without uncertainty, which is 19.36 % higher than the normal operation mode. In the TTSSUC method, the value of the operation cost of the system during 24 hours is 596375 $ for the mode with uncertainty and 596070 $ for the mode without uncertainty, which is 16.24 % higher than the normal operation mode.

Table 14. The operation cost of the system and the operation cost of the thermal units in the entire period of operation as well as the costs of load interruption contracts and adaptive frequency load shedding in the hours after the accident in Case Study 3 for both TTSSUC and proposed R-UCP methods

		R-UCP method				TTSSUC method			
		The operation cost of the system	The operation cost of the thermal units	The costs of load interruption contracts	The costs due to adaptive frequency load shedding	The operation cost of the system	The operation cost of the thermal units	The costs of load interruption contracts	The costs due to adaptive frequency load shedding
cost ($)	With uncertainty	612371	449473	86255	76643	596375	359452	89537	147386
	Without uncertainty	612037	449265	86457	76315	596070	359147	89537	147386

It should be noted that the operation cost of the system in the proposed R-UCP method for the scheduling the thermal units depends on the number and production capacity of the lost units and differs from the operation cost of the system in the normal mode. In normal operation, the purpose of the system operator is to respond 100 % to all consumers with the minimum operating cost. However, in the proposed R-UCP method, the aim is to increase resilience in the event of an incident, to reduce the consequences of sudden outage of production units, and prevent system frequency instability along with the maximum possible response to demand. According to the results of all the three case studies, it is observed that the proposed R-UCP method has a much better performance than the TTSSUC method.

4.4. Comparison of the results of methods in modes with uncertainty and without uncertainty for all case studies

Figure 3 shows the operation cost of the system and the operation cost of the thermal units for both methods, considering all the constraints during 24 hours for all case studies in both modes, with uncertainty and without uncertainty. Figure 4 shows the value of load interruption in

the load interruption contracts at each hour after the incident for all case studies for both TTSSUC and proposed R-UCP methods. Figure 5 shows the value of load shedding in the adaptive frequency load shedding at each hour after the incident for all case studies for both TTSSUC and proposed R-UCP methods. According to Figure 3, it is clear that the operation cost of the system and the operation cost of the thermal units in both methods are almost the same for all case studies in both modes with and without uncertainty. On the other hand, according to Figures 4 and 5, it can be seen that the value of load interruption in load interruption contracts and the value of load shedding in the adaptive frequency load shedding in each hour after the incident for all case studies in mode with uncertainty are different from the mode without uncertainty.

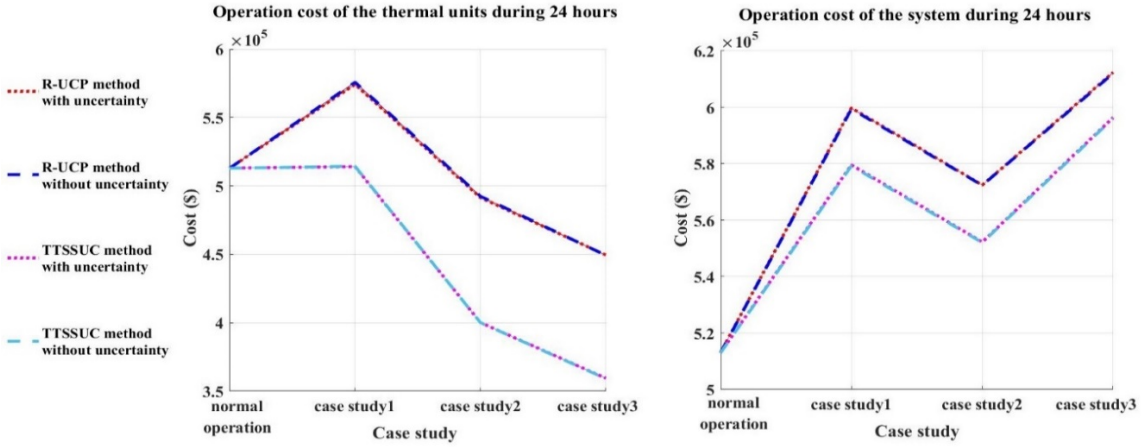

Figure 3. The operation costs of the system and the thermal units during 24 hours for both of the two methods

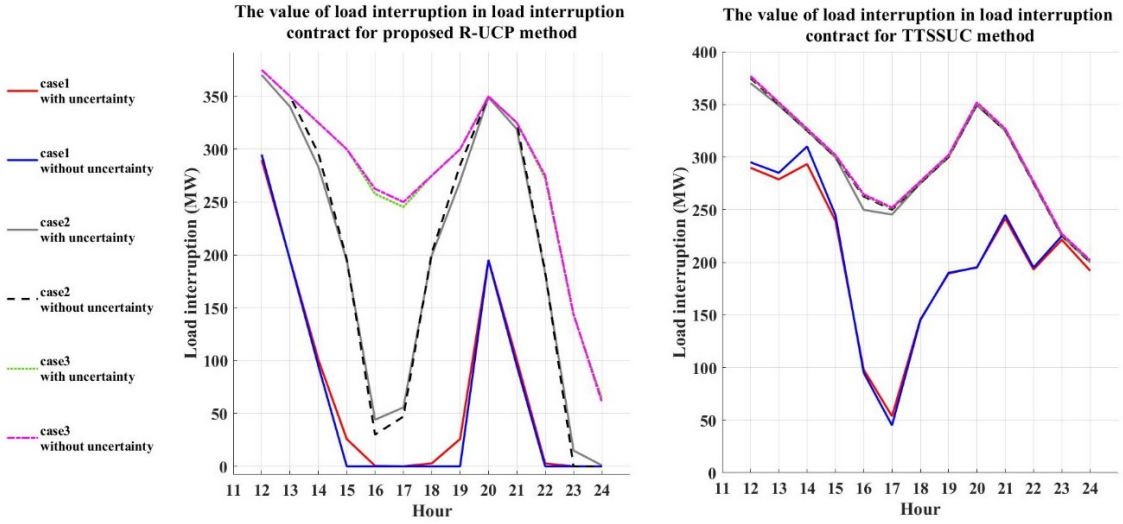

Figure 4. The value of load interruption in the load interruption contracts in each hour after the incident

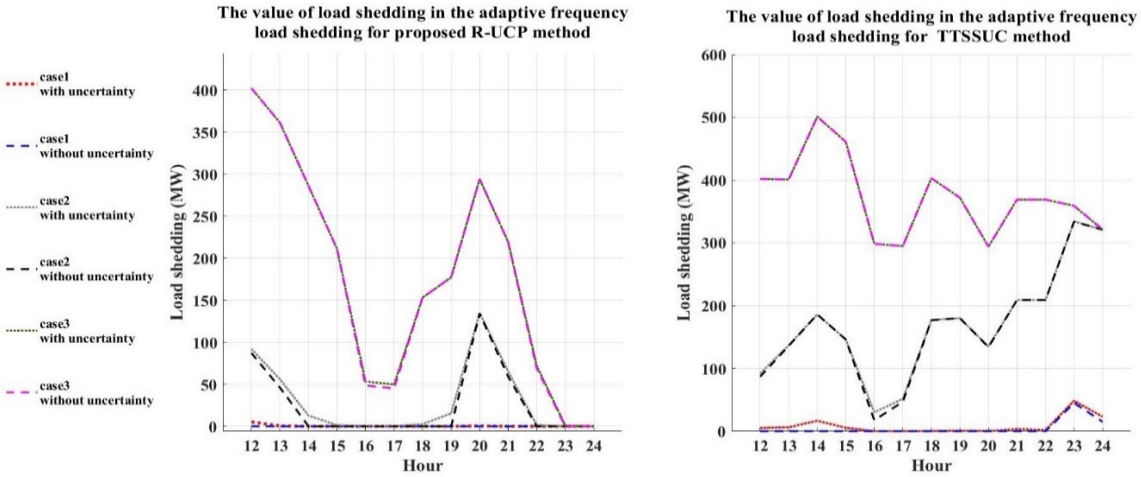

Figure 5. The value of load shedding in the adaptive frequency load shedding in each hour after the incident

Therefore, in both methods, if the objective is only to determine the operation costs of the system and thermal units, the existing uncertainties can be ignored for simplicity of calculations. However, in addition to calculating the operation cost of the system, it is necessary to accurately calculate and determine the value of load interruption in load interruption contracts and load shedding in adaptive frequency load shedding. Therefore, according to the given explanations, in the proposed R-UCP method employed for accurate scheduling of the system in the hours after the accident, the existing uncertainties must be carefully considered.

5. CONCLUSIONS

In this study, an R-UCP model was introduced along with the existing uncertainties. In this model, in the event of an accident using the production capacity, load interruption contracts, and adaptive frequency load shedding, system frequency instability and widespread unwanted load shedding in the system were prevented. In this model, the frequency change rate was introduced as a new resilience index. According to the results of case studies, in the proposed RUCP method, the value of unwanted load shedding in each hour after the incident in all case studies was much less than that in the case of the TTSSUC method. Therefore, the proposed R-UCP method was much more powerful for system scheduling in the hours after an incident than the widely used TTSSUC method.

According to the obtained results in Case Study 3, with the occurrence of the most destructive incident at peak load time, the proposed R-UCP method in the hours after the incident used the entire production capacity, the maximum value of load interruption contracts, and adaptive frequency load shedding. In this case study, the R-UCP method at the peak load time with only 19.36 % increase in the operation cost of the system compared to the normal operation mode and with a maximum value of unwanted load shedding equal to 26.8 % of the system load at peak hours managed to well prevent widespread unwanted load shedding and system frequency instability. However, in this case study, the minimum value of unwanted load shedding in the TTSSUC method was equal to the maximum value of unwanted load shedding in the proposed method. Also, the results of Case Studies 1 and 2 show that the presence of WSPP had a significant impact on reducing the operation cost of the system.

According to the results obtained by the R-UCP method, the system operator must carefully consider the existing uncertainties to accurately schedule the system in the hours after the incident. Upon comparing R-UCP with TTSSUC, it can be concluded that the proposed RUCP method is very powerful as a temporary scheme to maintain system frequency and reduce unwanted load shedding until the lost units are ready to be used again.

6. ACKNOWLEDGEMENT

The authors wish to thank the support of Razi University.

NOMENCLATURE

a_g	Constant coefficient of the quadratic production cost function of unit g ($/h)
b_g	First-order coefficient of the quadratic production cost function of the unit g ($/MWh)
c_g	Second-order coefficient of the quadratic production cost function of the unit g ($/MW^{2}h)
CSH_g	The maximum permissible time that the unit g has been offline to become hot (h)
DTi_g	The number of hours that the unit g has been shut down before the startup (h)
SU_g/SD_g	Startup/Shutdown ramp limit of unit g
RU_g	Ramp-up limit of unit g
UT_g	Minimum up-time of unit g (h)
DT_g	Minimum down-time of unit g (h)
Pw,t,φ	The mean predicted output power of wind power plant connected to the system at time t and in scenario φ (MW)
Ps,t,φ	The mean predicted output power of solar power plant connected to the system at time t and in scenario φ (MW)
Ug,t	State of unit g at hour t
P_t^D	Forecasted load demand at hour t (MW)
SR_t	Spinning reserve requirement at period t (MW)

Greek letters

α_g	Constant coefficient of the emission production function of unit g (ton/h)
β_g	First-order coefficient of the emission production function of unit g (ton/MWh)
γ_g	Second-order coefficient of the emission production function of unit g (ton/ MW^{2}h)
$P\varphi$	Probability of occurrence of scenario φ

REFERENCES

1. Khani, K., Shahgholian, Gh., Fani, B., Moazzami, M., Mahdavian, M. and Janghorbani, M., "A comparsion of different structures in wind energy conversion systems", ***Proceedings of 14th International Conference on Electrical Engineering/Electronics, Computer, Telecommunications and Information Technology (ECTI-CON)***, Phuket, Thailand, (2017), 58-61. (https://doi.org/10.1109/ECTICon.2017.8096172).
2. Wang, J., Zobaa, A.F., Huang, C. and Chen, C., "Day-ahead allocation of operation reserve in composite power systems with large-scale centralized wind farms", ***Journal of Modern Power Systems and Clean Energy***, Vol. 4, No. 2, (2016), 238-247. (https://doi.org/10.1007/s40565-015-0149-4).
3. Hosseini, E., Shahgholian, Gh., Mahdavi-Nasab, H. and Mesrinejad, F., "Variable speed wind turbine pitch angle control using three-term fuzzy controller", ***International Journal of Smart Electrical Engineering***, Vol. 11, No. 2, (2022), 63-70. (http://ijsee.iauctb.ac.ir/article_686590.html).
4. Huang, Y., Pardalos, P.M. and Zheng, Q.P., Electrical power unit commitment: Deterministic and two-stage stochastic programming models and algorithms, Springer, (2017), 50-80. (https://doi.org/10.1007/978-1-4939-6768-1).
5. Scuzziato, M.R., Finardi, E.C. and Frangioni, A., "Solving stochastic hydrothermal unit commitment with a new primal recovery technique based on Lagrangian solutions", ***International Journal of Electrical Power & Energy Systems***, Vol. 127, (2021), 1-11. (https://doi.org/10.1016/j.ijepes.2020.106661).
6. Li, G., Li, G. and Zhou, M., "Model and application of renewable energy accommodation capacity calculation considering utilization level of inter-provincial tie-line", ***Protection and Control of Modern Power Systems***, Vol. 4, No. 1, (2019), 1-12. (https://doi.org/10.1186/s41601-019-0115-7).
7. Håberg, M., "Fundamentals and recent developments in stochastic unit commitment", ***International Journal of Electrical Power & Energy Systems***, Vol. 109, (2019), 38-48. (https://doi.org/10.1016/j.ijepes.2019.01.037).
8. Mohammadi, F. and Ardakani, M.S., "Tractable stochastic unit commitment for large systems during predictable hazards", ***IEEE Access***, Vol. 8, (2020), 115078-115088. (https://doi.org/10.1109/ACCESS.2020.3004391).
9. Gholami, A., Shekari, T., Aminifar, F. and Shahidehpour, M., "Microgrid scheduling with uncertainty: The quest for resilience", ***IEEE Transactions on Smart Grid***, Vol. 7, No. 6, (2016), 2849-2858. (https://doi.org/10.1109/TSG.2016.2598802).
10. Gholami, A., Aminifar, F. and Shahidehpour, M., "Front lines against the darkness: Enhancing the resilience of the electricity grid through microgrid facilities", ***IEEE Electrification Magazine***, Vol. 4, No. 1, (2016), 18-24. (https://doi.org/10.1109/MELE.2015.2509879).
11. Fesagandis, H.S., Jalali, M., Zare, K., Abapour, M. and Karimipour, H., "Resilient scheduling of networked microgrids against real-time

failures", ***IEEE Access,*** Vol. 9, (2021), 21443-21456. (https://doi.org/10.1109/ACCESS.2021.3052653).

12. Mishra, D.K., Ghadi, M.J., Azizivahed, A., Li, L. and Zhang, J., "A review on resilience studies in active distribution systems", ***Renewable and Sustainable Energy Reviews***, Vol. 135, (2021), 1-20. (https://doi.org/10.1016/j.rser.2020.110201).
13. Ezzeldin, M. and El-dakhakhni, W.E., "Robustness of Ontario power network under systemic risks", ***Sustainable and Resilient Infrastructure***, Vol. 6, No. 3-4, (2019), 252-271. (https://doi.org/10.1080/23789689.2019.1666340).
14. Li, B., Boateng, D.O., Gel, Y.R. and Zhang, J., "A hybrid approach for transmission grid resilience assessment using reliability metrics and power system local network topology", ***Sustainable and Resilient Infrastructure***, Vol. 6, No. 1-2, (2021), 26-41. (https://doi.org/10.1080/23789689.2019.1708182).
15. Gholami, A., Shekari, T. and Grijalva, S., "Proactive management of microgrids for resiliency enhancement an adaptive robust approach", ***IEEE Transactions on Sustainable Energy***, Vol. 10, No. 1, (2019), 470-480. (https://doi.org/10.1109/TSTE.2017.2740433).
16. Chen, P.C. and Kezunovic, M., "Fuzzy logic approach to predictive risk analysis in distribution outage management", ***IEEE Transactions on Smart Grid***, Vol. 7, No. 6, (2016), 2827–2836. (https://doi.org/10.1109/TSG.2016.2576282).
17. Trakas, D.N. and Hatziargyriou, N.D., "Resilience constrained day-ahead unit commitment under extreme weather events", ***IEEE Transactions on Power Systems***, Vol. 35, No. 2, (2019), 1242-1253. (https://doi.org/10.1109/TPWRS.2019.2945107).
18. Zheng, Q.P., Wang, J. and Liu, A.L., "Stochastic optimization for unit commitment—A review", ***IEEE Transactions on Power Systems***, Vol. 30, No. 4, (2015), 1913-1924. (https://doi.org/10.1109/TPWRS.2014.2355204).
19. Cao, Y., Huang, L., Li, Y., Jermsittiparsert, K., Nezamabad, H.A. and Nojavan, S., "Optimal scheduling of electric vehicles aggregator under market price uncertainty using robust optimization technique", ***International Journal of Electrical Power & Energy Systems***, Vol. 117, (2020), 1-7. (https://doi.org/10.1016/j.ijepes.2019.105628).
20. Shahgholian, Gh., "A brief review on microgrids: Operation, applications, modeling, and control", ***Electrical Energy Systems***, Vol. 31, No. 6, (2021), 1-28. (https://doi.org/10.1002/2050-7038.12885).
21. Marzband, M., Moghaddam, M.M., Akorede, M.F. and Khomeyrani, G., "Adaptive load shedding scheme for frequency stability enhancement in microgrids", ***Electric Power Systems Research***, Vol. 140, (2016), 78-86. (https://doi.org/10.1016/j.epsr.2016.06.037).
22. Choopani, K., Effatnejad, R. and Hedayati, M., "Coordination of energy storage and wind power plant considering energy and reserve market for a resilience smart grid", ***Journal of Energy Storage***, Vol. 30, (2020), 1-8. (https://doi.org/10.1016/j.est.2020.101542).
23. Vahedipour, M., Moghaddam, A.A. and Guerrero, J.M., "Evaluation of reliability in risk-constrained scheduling of autonomous microgrids with demand response and renewable resources", ***IET Renewable Power Generation***, Vol. 12, No. 6, (2018), 657-667. (https://doi.org/10.1049/iet-rpg.2017.0720).
24. Wang, Y., Huang, L., Shahidehpour, M., Lai, L.L. and Zhou, Y., "Impact of cascading and common-cause outages on resilience-constrained optimal economic operation of power systems", ***IEEE Transactions on Smart Grid***, Vol. 11, No. 1, (2020), 590-601. (https://doi.org/10.1109/TSG.2019.2926241).
25. Eskandarpour, R., Khodaei, A. and Lin, J., "Event-driven security constrained unit commitment with component outage estimation based on machine learning method", ***Proceedings of the North American Power Symposium (NAPS)***, Denver, CO, USA, (2016), 1-6. (https://doi.org/10.1109/NAPS.2016.7747873).
26. hao, T., Zhang, H., Liu, X., Yao, S. and Wang, P., "Resilient unit commitment for day-ahead market considering probabilistic impacts of hurricanes", ***IEEE Transactions on Power Systems***, Vol. 36, No. 2, (2021), 1082-1094. (https://doi.org/10.1109/TPWRS.2020.3025185).
27. Wang, Y., Li, Z., Shahidehpour, M., Wu, L., Guo, C.X. and Zhu, B., "Stochastic co-optimization of midterm and short-term maintenance outage scheduling considering covariates in power systems", ***IEEE Transactions on Power Systems***, Vol. 31, No. 6, (2016), 4795-4805. (https://doi.org/10.1109/TPWRS.2016.2521720).
28. Sayyed-Mahdavi, S. and Javidi, M.H., "VPP decision making in power markets using benders decomposition", ***International Transactions on Electrical Energy Systems***, Vol. 24, No. 7, (2014), 960-975. (https://doi.org/10.1002/etep.1748).
29. Mohammadi, F., Sahraei-Ardakani, S., Trakas, D. and Hatziargyriou, N.D., "Machine learning assisted stochastic unit commitment during hurricanes with predictable line outages", ***IEEE Transactions on Power Systems***, Vol. 36, No. 6, (2021), 5131-5142. (https://doi.org/10.1109/TPWRS.2021.3069443).
30. Zakariazadeh, A., Jadid, S. and Siano, P., "Economic-environmental energy and reserve scheduling of smart distribution systems: A multi objective mathematical programming approach", ***Energy Conversion and Management***, Vol. 78, (2014), 151-164. (https://doi.org/10.1016/j.enconman.2013.10.051).
31. Reddy, S.S., Bijwe, P.R. and Abhyankar, A.R., "Joint energy and spinning reserve market clearing incorporating wind power and load forecast uncertainties", ***IEEE Systems Journals***, Vol. 9, No. 1, (2015), 152-164. (https://doi.org/10.1109/JSYST.2013.2272236).
32. Arab, A., Khodaei, A., Khator, S.K. and Han, Z., "Electric power grid restoration considering disaster economics", ***IEEE Access***, Vol. 4, (2016), 639-649. (https://doi.org/10.1109/ACCESS.206.2523545).
33. Roy, P.K., "Solution of unit commitment problem using gravitational search algorithm", ***International Journal of Electrical Power & Energy Systems***, Vol. 53, (2013), 85-94. (https://doi.org/10.1016/j.ijepes.2013.04.001).
34. Govardhan, M. and Roy, R., "Economic analysis of unit commitment with distributed energy resources", ***International Journal of Electrical Power & Energy Systems***, Vol. 71, (2015), 1-14. (https://doi.org/10.1016/j.ijepes.2015.01.028).
35. Mahmutoğulları, A.I., Ahmed, S., Çavuş, Ö. and Aktürk, M.S., "The value of multi-stage stochastic programming in risk-averse unit commitment under uncertainty", ***IEEE Transactions on Power Systems***, Vol. 4, No. 5, (2019), 3667-3676. (https://doi.org/10.1109/TPWRS.2019.2902511).
36. Tielens, P. and Hertem, D., "Grid inertia and frequency control in power systems with high penetration of renewables", ***Proceedings of the Young Researchers Symposium in Electrical Power Engineering***, Delft, Netherlands, (2012), 1-6. (https://lirias.kuleuven.be/1731030?limo=0).
37. Carrión, M. and Arroyo, J.M., "A computationally efficient mixed-integer linear formulation for the thermal unit commitment problem", ***IEEE Transactions on Power Systems***, Vol. 21, No. 3, (2006), 1371-1378. (https://doi.org/10.1109/TPWRS.2006.876672).
38. Venkatesan, T. and Sanavullah, M.Y., "SFLA approach to solve PBUC problem with emission limitation ", ***International Journal of Electrical Power & Energy Systems,*** Vol. 46, (2013), 1-9. (https://doi.org/10.1016/j.ijepes.2012.09.006).
39. Elia Power System, (2021). (http://www.elia.be/en/grid-data/powergeneration), (Accessed: 11 November 2021).
40. Wan, Y.H., "Wind power plant behaviors: Analyses of long-term wind power data", National Renewable Energy Laboratory (NREL) Report, Golden, CO, USA, (2004). (https://www.osti.gov/biblio/15009608), (Accessed: 1 September 2004).
41. Hummon, M., Cochran, J., Weekley, A., Lopez, A., Zhang, J. and Stoltenberg, B., "Variability of photovoltaic power in the state of gujarat using high resolution solar data", National Renewable Energy Laboratory (NREL) Report, Golden, CO, USA, (2014). (https://www.osti.gov/biblio/1126817), (Accessed: 1 March 2014).
42. Wood, A.J., Wollenberg, B.F. and Sheblé, G.B., Power generation, operation, and control, John Wiley & Sons, (2013), 147-167. (https://www.amazon.com/Power-Generation-Operation-Control-Allen/dp/0471790559).